[CANCER RESEARCH 61, 8498–8503, December 1, 2001]

MIG (CXCL9) Chemokine Gene Therapy Combines with Antibody-Cytokine Fusion Protein to Suppress Growth and Dissemination of Murine Colon Carcinoma[1]

J. Michael Ruehlmann, Rong Xiang, Andreas G. Niethammer, Yi Ba, Ursula Pertl, Carrie S. Dolman, Stephen D. Gillies, and Ralph A. Reisfeld[2]

The Scripps Research Institute, Department of Immunology, La Jolla, California 92037 [J. M. R., R. X., A. G. N., Y. B., U. P., C. S. D., R. A. R.], and Lexigen Pharmaceuticals Corp., Lexington, Massachusetts 02173 [S. D. G.]

ABSTRACT

The induction of a CTL response capable of eradicating disseminated tumor metastases and the establishment of a persistent tumor-protective immunity remain major goals of cancer immunotherapy. Here, we demonstrate for the first time that the combination of interleukin 2 (IL-2) targeted to the tumor microenvironment by a recombinant antibody-IL-2 fusion protein (huKS1/4-IL-2) with gene therapy by the murine chemokine *MIG* (CXCL9) markedly reduced s.c. tumor burden and decisively suppressed dissemination of experimental lung metastases of CT26-KSA colon carcinoma in syngeneic BALB/c mice. This combined therapy significantly prolonged the life span of these mice 3–4-fold by concurrently delivering MIG and IL-2 to the tumor site and thereby achieving chemoattraction of T cells together with their activation. The antitumor effect obtained was mediated predominantly by MHC class I antigen-restricted $CD8^+$ T cells with help from MHC class II antigen-restricted $CD4^+$ T lymphocytes. In addition, the MIG chemokine also induced angiostatic effects in the tumor vasculature. Taken together, this combination of *MIG* chemokine gene therapy with tumor-targeted cytokine IL-2 provides an approach for the rational design of novel cancer immunotherapy modalities.

INTRODUCTION

The possibility to effectively modify and enhance immune responses against infectious and malignant diseases has become a major focus of interest for the development of novel treatment modalities. In this regard, the application of cytokines and chemokines was demonstrated to be beneficial in a large number of experimental animal models of infectious and malignant diseases (1, 2), and has become an alternative or an addendum to chemotherapy in the treatment of some human malignancies. Thus, cytokines such as IL-2[3] (3), IL-12 (4, 5), IFN-α, and IFN-γ (6) were found useful in the treatment of renal cell carcinoma (7) and melanoma (8). Other potential candidates for such immunotherapeutic interventions are chemokines, known to chemoattract specific leukocyte subpopulations to sites of infection or the tumor microenvironment (9). However, chemokines and chemokine receptors have been studied mainly in infectious diseases, particularly HIV and AIDS, whereas relatively little is known about their role in cancer therapy (10, 11). Chemokines, extensively described in several recent reviews (12–14), represent an extended family of cytokine-inducible secreted proteins of low molecular weight, which are characterized by four invariant cysteine residues at their NH_2 termini (12). Among a variety of chemokines, MIG, *i.e.*, monokine induced by IFN-γ (14–16), is a member of the CXC (α-) subfamily, characterized by its first two cysteines being separated by a single amino acid. Important for our purpose, the M_r 12,000 chemokine MIG functions *in vivo* as a potent chemoattractant for tumor-infiltrating lymphocytes (17), activated peripheral blood lymphocytes (12), as well as NK cells and T_{H1} lymphocytes (18). Among the CXC chemokines, MIG belongs to a subgroup lacking the characteristic, proangiogenic ELR-motif and, thus, functions as an angiostatic agent (19). MIG is also known to promote tumor necrosis when administered intratumorally (20). CXCR3 serves as the receptor for MIG, which is expressed exclusively on T and NK cells after activation by IFN-γ (13) but is absent from resting T or B lymphocytes as well as monocytes and granulocytes (21).

On the basis of our earlier application of the recombinant antibody-IL-2 fusion protein (huKS1/4-IL-2) in the treatment of murine colon carcinoma (22–24), we now combined both gene therapy by the CXC chemokine *MIG* with immunotherapy by the huKS1/4-IL-2 fusion protein, which targets IL-2 specifically to the tumor microenvironment.

MATERIALS AND METHODS

Construction of an Expression Plasmid Encoding mMIG (CXCL9). The murine *MIG* gene was cloned by RT-PCR using murine splenocytes as a template that were prestimulated for 48 h with ConA. The following primers were used: CGGGGTA CCGCCACCATGAAGTCCGCTGTTCTTTTC (forward); and ACGTCTAGATGTAGTCT TCCTTGAACGACG (reverse). The design of these primers results in cloning of the *mMIG* gene downstream of the Kozak sequence (25, 26), which is required for the initiation of transcription. Using *Kpn*I and *Xba*I as restriction sites, this construct was inserted into the plasmid pcDNA3.1(+; Invitrogen, Carlsbad, CA), which was subsequently used for transfection of the murine colon carcinoma cell line CT26-KSA.

Cell Lines. The murine colon carcinoma cell line CT26, kindly provided by Dr. Isaiah J. Fidler, M.D. Anderson Cancer Center, Houston, TX, was described previously (22, 23). This cell line was stably transfected with the human epithelial cell adhesion molecule EpCAM/KSA to provide a docking site for the huKS1/4-IL-2 fusion protein (27). Additionally, the CT26-KSA cell line was also stably transfected with the gene encoding the murine chemokine MIG with the LipofectAMINE transfection system (Life Technologies, Inc., Grand Island, NY). Positive clones were selected by using 200 μg/ml zeocin (Invitrogen). All of the cell lines used were analyzed periodically and tested negatively for *Mycoplasma*.

RT-PCR. Total RNA was extracted from 3×10^6 double-transfected colon carcinoma cells CT26-KSA-MIG using the RNeasy Mini kit (Qiagen, Valencia, CA). Reverse transcription was performed with 1 μg of total RNA followed by PCR with the same oligonucleotides as described above. The PCR was cycled 30 times at an annealing temperature of 60°C to result in a 380-bp fragment. RNA quantity and PCR were monitored by PCR for glyceraldehyde-3-phosphate dehydrogenase resulting in a 295-bp fragment.

Western Blot Analysis. To detect protein production, COS-7 kidney cells were transfected with the plasmid encoding the murine *MIG* gene using a calcium phosphate transfection kit (Invitrogen) following the manufacturer's instructions. After 48 h, COS-7 and COS-7-MIG cells were harvested for the detection of protein expression. Western blot analysis was done with total protein of cell lysate homogenates using a polyclonal primary rabbit antibody directed against murine MIG (kindly provided by Dr. Lili Feng, The Scripps Research Institute). Specific protein was detected by a goat antirabbit, horseradish-peroxidase conjugated IgG antibody (Calbiochem, La Jolla, CA).

Received 7/20/01; accepted 10/3/01.

The costs of publication of this article were defrayed in part by the payment of page charges. This article must therefore be hereby marked *advertisement* in accordance with 18 U.S.C. Section 1734 solely to indicate this fact.

[1] Supported by NIH Grant CA83856 (to R. A. R.) and a Cancer Research Fund Grant under Interagency Agreement 211-0020 (University of California, Davis contract 00-0078V) with the Department of Health Services, Cancer Research Section (to R. A. R.). J. M. R. is a fellow of the Deutsche Forschungsgemeinschaft and A. G. N. is a fellow of the Deutsche Krebshilfe. This is The Scripps Research Institute's manuscript number 14220-IMM.

[2] To whom reprint requests should be addressed, at: The Scripps Research Institute, Department of Immunology, La Jolla, CA 92037. E-mail: reisfeld@scripps.edu.

[3] The abbreviations used are: IL, interleukin; NK, natural killer; RT-PCR, reverse transcription-PCR; rhIL-2, recombinant human IL-2; mAb, monoclonal antibody.

Migration Assay. To assess the chemoattractive properties of MIG we used cell culture supernatants harvested from CT26-KSA and CT26-KSA-MIG tumor cells after 72 h of fetal bovine serum-deprivation. Migration of splenocytes was evaluated in a 24-well chemotaxis chamber. The lower wells of these chambers were filled with 600 μl of supernatants obtained as described above. A 5-μm pore size, fibronectin coated Transwell Polycarbonate Membrane (Costar, Cambridge, MA), was placed above the wells and then 100-μl of cell suspension (1×10^7 splenocytes/ml migration medium) was added to the upper compartment of the migration chamber and incubated for 5 h at 37°C in a humidified CO_2 incubator. Cells that had migrated through the polycarbonate membrane were harvested from the lower chamber and counted under a microscope. Results are expressed as the mean value of triplicates ± SD; the assay was repeated three times with a variability of <10%.

Animal Experiments. Tumors were generated by s.c. injection of 5×10^5 tumor cells in 100 μl of PBS into the left flank of 6–8-week-old syngeneic, female BALB/c mice. Subsequent tumor size was measured by caliper and the tumor volume calculated using the formula ½(length^2 × width). Subcutaneous tumors were treated by i.v. injections of 5 μg of huKS1/4-IL-2 fusion protein each on days 1–5 after tumor cell inoculation. The humanized antibody was constructed as described previously (28) as was the fusion protein (27–29). A chimeric antibody-cytokine fusion protein was applied to reduce the formation of murine antihuman antibodies. This chimeric fusion protein is well tolerated for at least 7 consecutive i.v. applications of ≤20 μg fusion protein/injection (data not shown).

Survival studies were initiated by inducing experimental pulmonary metastases after i.v. injection of 5×10^4 cells in 100 μl of PBS into 6–8-week-old syngeneic, female BALB/c mice. Established metastases were treated with subcurative doses of six i.v. injections of 5 μg/day of huKS1/4-IL-2 fusion protein on days 4–9 after tumor cell inoculation. Two control groups of mice received a mixture of 5 μg/day huKS1/4 mAb and 15,000 IU rhIL-2, a dose equivalent to that applied with 5 μg/day of the huKS1/4-IL-2 fusion protein. For immunohistochemical staining, tumor-bearing mice were sacrificed on day 12 and lungs removed and snap frozen. Each experimental group consisted of 8–10 BALB/c mice. All of the animal experiments were performed in compliance with the NIH Guide for the Care and Use of Laboratory Animals and approved by The Scripps Research Institute.

***In Vivo* Depletion of CD4$^+$ or CD8$^+$ T Lymphocytes.** As described earlier (22), female BALB/c mice were depleted of CD4$^+$ or CD8$^+$ T lymphocyte subsets using rat IgG_{2b} antimurine CD4 (clone GK1.5; National Cell Culture Center, Minneapolis, MN) or rat IgG_{2b} antimurine CD8 (clone 2.43; National Cell Culture Center) antibodies, respectively. Depletion was achieved by i.p. injections of 500 μg each of anti-CD4- or anti-CD8-specific mAbs on days −4, −1, 2, 6, 10, and 14. FACS analyses of lymph node- and spleen-derived lymphocytes confirmed the depletion of >95% of the respective T-cell subsets before the treatment of mice was initiated.

Cytotoxicity Assay. Cytotoxicity was measured in a standard ^{51}Cr-release assay with CT26-KSA cells serving as target cells. Effector cells were isolated from spleens of BALB/c mice bearing pulmonary metastases 3 days after cessation of therapy. Coincubation of effector and target cells (5×10^3) at 37°C was done at different E:T ratios for 4 h. To investigate the MHC class I and class II antigen-dependent inhibition of cytotoxicity, 40 μg/ml of antimouse MHC antigen class I (H-2K^d; PharMingen, San Diego, CA) and antimouse MHC antigen class II (I-A^d/I-E^d; PharMingen) antibodies were used. Nonspecific antibodies, directed against H-2D^b and H-2K^b failed to inhibit cytotoxicity (data not shown). The percentage of specific CT26-KSA target cell lysis was calculated using the formula [(E-S)/(T-S)] × 100 with E being the average experimental release, S the average spontaneous release, and T the average total release.

***In Vivo* Matrigel Plug Angiogenesis Assay.** Liquefied Matrigel (400 μl/mouse; Becton Dickinson, Bedford, MA) mixed with 1×10^5 CT26-KSA or CT26-KSA-MIG tumor cells were injected s.c. into the flank of BALB/c mice. On day 6, mice were sacrificed and plugs removed, weighed, and fixed in 3.7% formaldehyde/PBS. The formation of blood vessels during tumor growth and the abrogation thereof by *MIG* chemokine gene therapy was quantified by determining the hemoglobin content of Matrigel plaques according to the methods described by Passaniti *et al.* (30) and Drabkin and Austin (31).

Immunohistochemical Analyses. Frozen sections of Matrigel were fixed in acetone, and endogenous peroxidase was removed by incubation with 0.03% H_2O_2. Nonspecific antibody binding was prevented by blocking with 10% species-specific serum in 1% BSA/PBS. Afterward, anti-CD8$^+$ (clone 2.43), anti-CD4$^+$ (clone GK1.5), and anti-CD31 (PharMingen) mAbs were overlaid onto serial sections at concentrations of 10–20 μg/ml for 30 min in a humid chamber at 37°C. Then the slides were incubated with a biotinylated secondary antibody for 10 min followed by exposure to either peroxidase or alkaline phosphatase-linked streptavidin.

Statistical Analyses. The statistical significance of findings in all of the experiments was determined by the two-tailed Student's *t* test. Findings were regarded as significant if two-tailed *P*s were <0.05.

RESULTS

Integrity and Function of the Murine MIG Construct. After insertion of the murine *MIG* gene into the expression vector pcDNA3.1, the integrity of the gene was confirmed by sequencing. RT-PCR using total RNA of transfected CT26-KSA-MIG cells confirmed the successful transfer of the murine *MIG* gene into this colon carcinoma cell line, whereas parental CT26-KSA cells did not reveal any signal for MIG (Fig. 1*A*). Western blot analysis of transfected COS-7 cell lysates revealed expression of a M_r 12,000 protein, which is the appropriate size for murine MIG (Fig. 1*B*). In addition, the migration assay (Fig. 1*C*) showed clearly that supernatants from CT26-KSA-MIG cells, in contrast to those from CT26-KSA cells, were able to induce the migration of murine splenocytes. The difference between experimental groups is statistically significant ($P < 0.01$).

The Combination of *MIG* Gene Therapy with huKS1/4-IL-2 Fusion Protein Therapy Suppresses s.c. Growth of CT26-KSA Colon Carcinoma. After s.c. injection of 5×10^5 CT26-KSA-MIG cells, tumors with an volume of ~450 mm^3 developed within 25 days (Fig. 2). In contrast, the same number of CT26-KSA cells formed tumors of ~1200 mm^3 during the same time period. Importantly, the

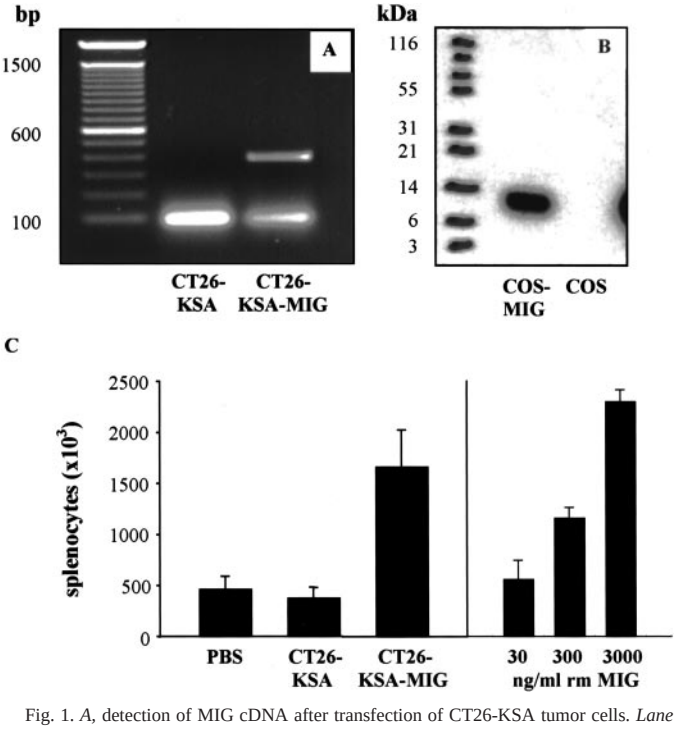

Fig. 1. *A*, detection of MIG cDNA after transfection of CT26-KSA tumor cells. *Lane 1* reveals analysis of parental CT26-KSA tumor cells; *Lane 2* indicates results obtained with CT26-KSA-MIG. *B*, detection of MIG protein by Western blotting after transfection of COS-7 cells. Results with COS-MIG cells are shown in *Lane 1* (40 μg protein) and with COS cells in *Lane 2*. *C*, enhanced migratory response of murine splenocytes toward supernatants of CT26-KSA-MIG cells compared with CT26-KSA controls. Data are shown as mean ($n = 3$); *bars*, ± SD. PBS was used as a negative control and recombinant murine MIG served as a positive control.

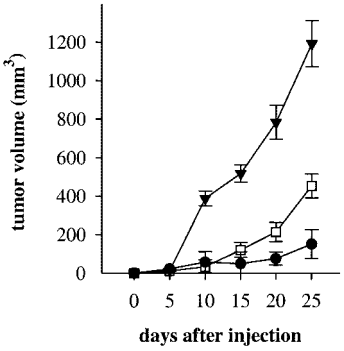

Fig. 2. Suppression of s.c. tumor growth in syngeneic BALB/c mice treated with *mMIG* gene therapy combined with huKS1/4-IL-2 fusion protein therapy. Comparisons are shown between CT26-KSA (▼); CT26-KSA-MIG (□); and CT26-KSA-MIG + huKS1/4-IL-2 fusion protein therapy (●). Data are shown as mean ($n = 6$); *bars*, ± SD. The statistical differences between CT26-KSA and CT26-KSA-MIG as well as between CT26-KSA-MIG and CT26-KSA-MIG + huKS1/4-IL-2 fusion protein therapy are $P < 0.0001$.

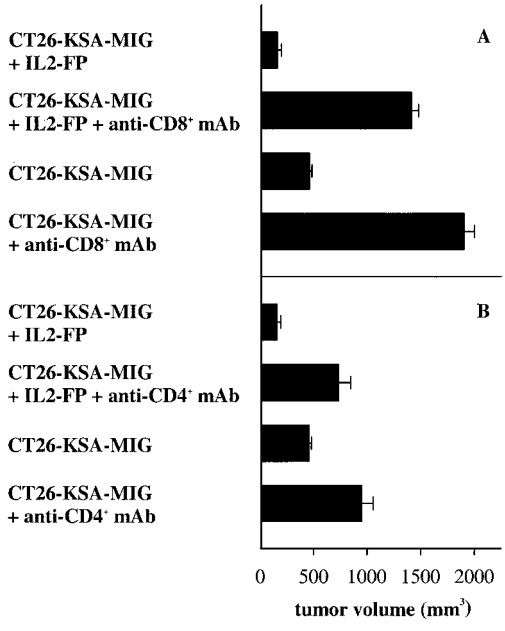

Fig. 3. Role of $CD8^+$ and $CD4^+$ T-effector cells in the suppression of s.c. tumor growth. Comparisons are shown between *mMIG* gene therapy (CT26-KSA-MIG) + huKS1/4-IL-2 fusion protein therapy (IL-2-FP) and *mMIG* gene therapy alone (CT26-KSA-MIG). Data are shown as mean ($n = 6$); *bars*, ± SD. Effect on treatment efficacy is indicated by *in vivo* depletion of (*A*) $CD8^+$ or (*B*) $CD4^+$ T lymphocytes.

combination of *mMIG* gene therapy with the i.v. application of humanized KS1/4-IL-2 fusion protein therapy strongly enhanced the effect of chemokine gene therapy *per se*, because the volume of s.c. growing tumors was additionally reduced from ~450 mm^3 to 150 mm^3 ($P < 0.001$) by the combination therapy.

To determine the role of effector T cells, we depleted mice of $CD8^+$ and $CD4^+$ T lymphocytes, respectively (Fig. 3). The depletion of $CD8^+$ T lymphocytes in mice that thereafter were injected with the CT26-KSA-MIG cell line resulted in a decisive 4-fold increase in s.c. tumor volumes within 25 days reaching up to 1900 mm^3. The subsequent treatment of $CD8^+$ T-cell-depleted mice with subcurative doses of huKS1/4-IL-2 fusion protein resulted in s.c. tumor volumes of 1400 mm^3 ($P < 0.001$). These data clearly indicate the critical role of $CD8^+$ T cells in the antitumor effects induced by *mMIG* gene therapy combined with huKS1/4-IL-2 fusion protein treatment. The depletion of $CD4^+$ T lymphocytes resulted in a doubling of s.c. tumor volumes within 25 days to 950 mm^3, and subsequent treatment of these mice with huKS1/4-IL-2 fusion protein resulted in an average tumor volume of 730 mm^3 ($P < 0.01$). These findings point to a critical role of $CD4^+$ T-cell help in the induction of the $CD8^+$ T-cell-mediated antitumor effect.

Prolongation of Survival by *MIG* Gene Therapy in Combination with huKS1/4-IL-2 Fusion Protein Therapy. To assess the efficacy of *MIG* gene therapy combined with huKS1/4-IL-2 fusion protein in a relevant minimal residual disease setting, we determined the life span of mice after treatment of their established experimental pulmonary metastases (Fig. 4). Control animals that received no treatment survived only an average of 26.9 days. In contrast, the combination of *mMIG* gene therapy with i.v. injections of 5 μg/day of huKS1/4-IL-2 fusion protein on days 4–9 after tumor cell inoculation resulted in a significant 3-fold increase in life span to >85 days in 100% of experimental animals (average survival: 108.8 days; $P < 0.0001$). Although 4 of 8 animals died between days 86 and 106 after tumor cell inoculation, the remaining 4 mice survived >108 days and, thus, attained a 4-fold increase in life span. In contrast, *MIG* gene therapy alone resulted only in an average life span of 33.5 days, whereas mice that received only subcurative doses of the huKS1/4-IL-2 fusion protein for 6 days survived 36.5 days. An additional control group of mice that received a mixture of 5 μg/day huKS1/4 mAb + 15,000 IU/day rhIL-2, a dose equivalent to that provided by 5 μg/day of huKS1/4-IL-2 fusion protein, reached only an average life span of 27.4 days. The combination of *mMIG* gene therapy with a mixture of huKS1/4 antibody and rhIL-2 cytokine had little effect and resulted in an average life span of 44.6 days. Taken together, the data from these experiments indicate that the combination of *mMIG* gene therapy plus the huKS1/4-IL-2 fusion protein was optimal, resulting in a 3-fold increase in life span to >85 days in 100% of mice and in a 4-fold increase in life span in 50% of experimental animals.

Effects of *MIG* Gene Therapy on Infiltration of Matrigel-embedded Tumor Cells by Immune Effector Cells. As documented in Fig. 5, chemokine gene therapy with m*MIG* leads to a marked increase in the number of $CD8^+$ and $CD4^+$ T lymphocytes (Fig. 5, *B* and *D*) infiltrating the Matrigel-embedded colon carci-

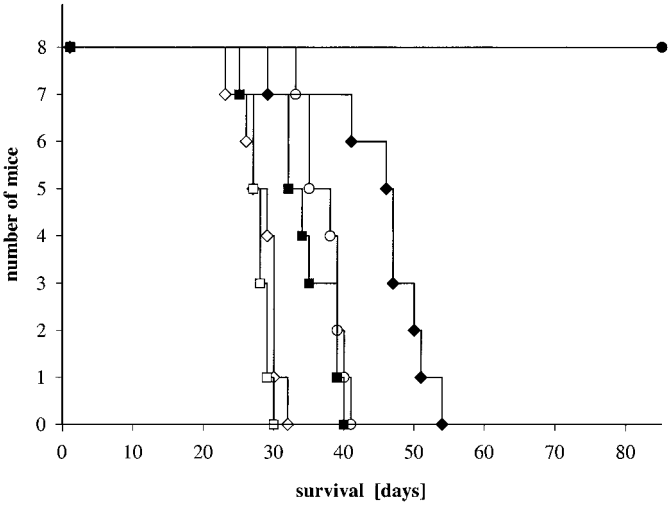

Fig. 4. Kaplan-Meier plot depicting the survival of syngeneic female BALB/c mice injected i.v. with 5×10^4 tumor cells in 100 μl of PBS. Established metastases were treated by i.v. injections of 5 μg of huKS1/4-IL-2 fusion protein on days 4–9 after tumor cell inoculation. CT26-KSA-MIG + 5 μg/day huKS1/4-IL-2 fusion protein therapy (●); CT26-KSA-MIG + 5 μg/day huKS1/4 mAb + 15000 IU/day rhIL-2 (♦); CT26-KSA-MIG + PBS (■); CT26-KSA + 5 μg/day huKS1/4-IL-2 fusion protein therapy (○); CT26-KSA + 5 μg/day huKS1/4 mAb + 15000 IU/day rhIL-2 (◇); and CT26-KSA + PBS (□). The statistical differences of life span between CT26-KSA and CT26-KSA-MIG as well as between CT26-KSA-MIG and CT26-KSA-MIG + huKS1/4-IL-2 fusion protein therapy are $P < 0.0001$.

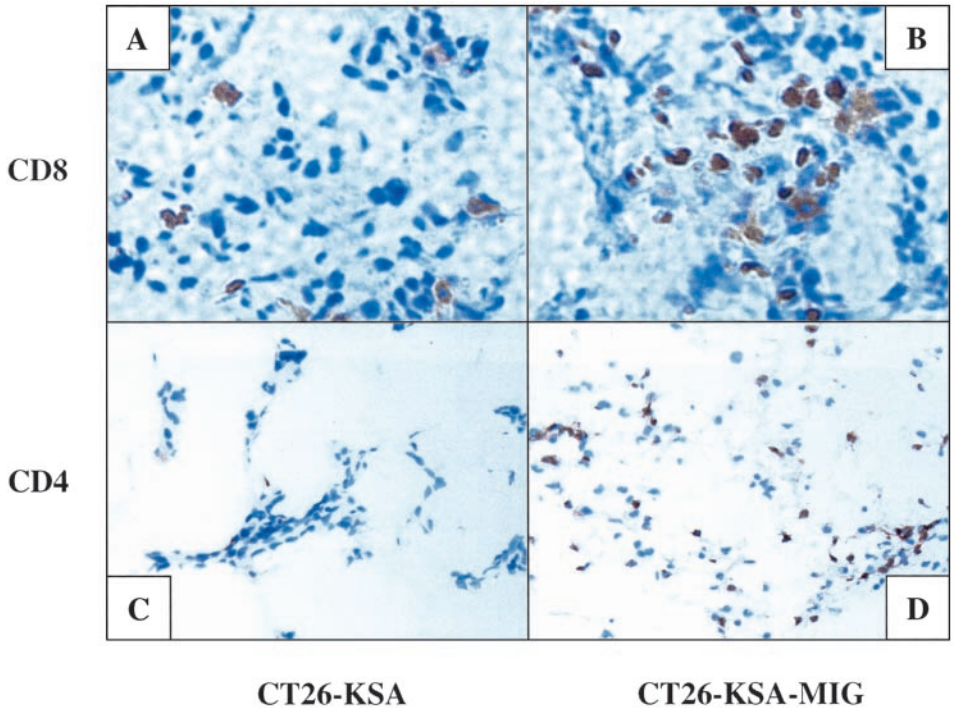

Fig. 5. Immunohistochemical staining of Matrigel-embedded, nontransfected CT26-KSA tumor cells (*A* and *C*) compared with *MIG* gene-transfected CT26-KSA-MIG tumor cells (*B* and *D*). Samples were stained for $CD8^+$ (*A* and *B*) and $CD4^+$ (*C* and *D*) T lymphocytes as described in "Materials and Methods."

noma cells in comparison with CT26-KSA wild-type tumor cells (Fig. 5, *A* and *C*). Furthermore, we also investigated the infiltration of Matrigel-embedded tumor cells by NK cells but did not find significant differences between MIG-transfected tumor cells and controls (data not shown).

Effects of *MIG* Gene Therapy on Neovascularization of Matrigel-embedded Tumor Cells. As documented by the data shown in Fig. 6, *MIG* chemokine gene therapy leads to a marked decrease in neovascularization of tumor cells embedded in Matrigel. This was shown by a decrease in the number of $CD31^+$ endothelial cells (Fig. 6*D*) compared with untreated controls (Fig. 6*C*). Additionally, H&E staining confirmed this angiostatic effect of MIG by indicating newly formed blood vessels in controls (Fig. 6*A*) that disappeared after *MIG* gene therapy (Fig. 6*B*).

As documented by the data shown in Fig. 6E, Matrigel plaques that contain CT26-KSA-MIG tumor cells display a lower content of hemoglobin than control Matrigel plaques that contain CT26-KSA tumor cells. The difference between our *MIG* gene therapy group and a control group is statistically significant ($P < 0.005$). As the hemoglobin content of Matrigel plaques parallels the neovascularization of Matrigel-embedded tumor cells, this finding provides additional evidence for the angiostatic effect of *MIG* gene therapy.

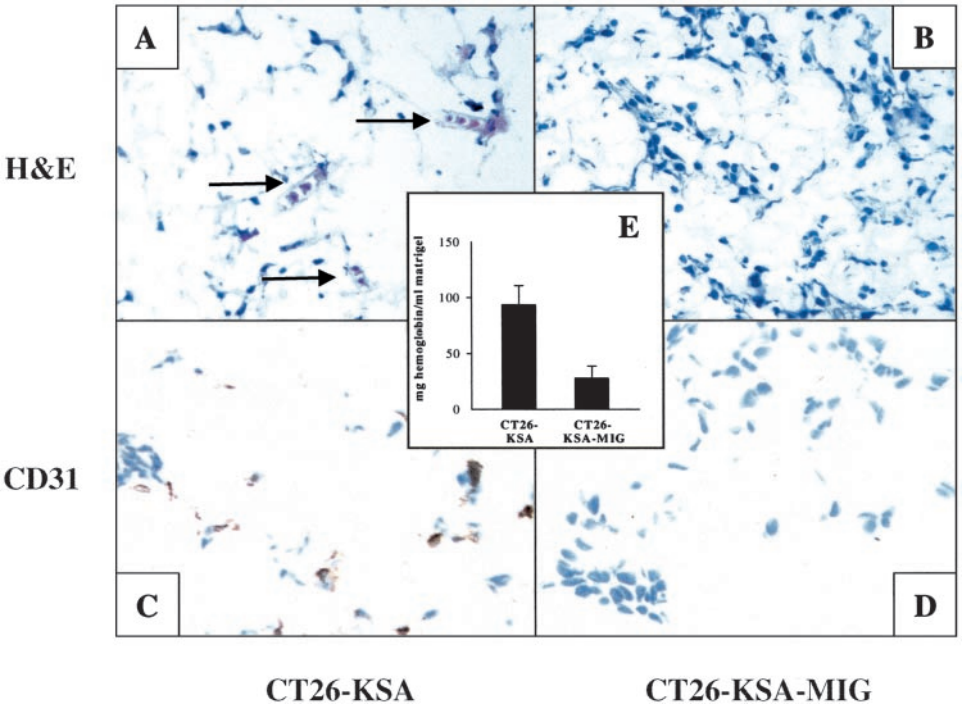

Fig. 6. H&E staining of Matrigel-embedded, nontransfected CT26-KSA tumor cells (*A*) compared with *MIG* gene-transfected CT26-KSA-MIG tumor cells (*B*) and CD31-immunostaining of Matrigel-embedded CT26-KSA tumor cells (*C*) compared with *MIG* gene-transfected CT26-KSA-MIG (*D*) as described in "Materials and Methods." *Arrows* point to newly formed blood vessels. *E*, hemoglobin content is shown in Matrigel plaques that contain CT26-KSA-MIG tumor cells in comparison with such plaques including CT26-KSA tumor cells. The statistical difference between experimental groups ($n = 4$) and controls is $P < 0.005$.

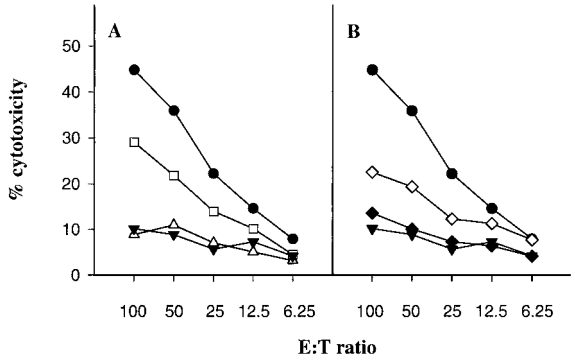

Fig. 7. Cytotoxicity induced by *MIG* gene therapy and enhanced by huKS1/4-IL-2 fusion protein therapy. Splenocytes were obtained from mice 3 days after cessation of the following therapies: *A*, CT26-KSA-MIG + huKS1/4-IL-2 fusion protein therapy (●); CT26-KSA-MIG (□); CT26-KSA (▼); and B16 melanoma (△). *B*, effect on cytotoxicity of coincubation with antibodies directed against MHC class I and class II antigens. CT26-KSA-MIG + huKS1/4-IL-2 fusion protein therapy (●); CT26-KSA (▼); CT26-KSA-MIG + huKS1/4-IL-2 fusion protein therapy + anti-MHC class I antibody (◆); and CT26-KSA-MIG + huKS1/4-IL-2 fusion protein therapy + anti-MHC class II antibody (◇).

Effect of Combination Therapy on CTL Activity. Cytotoxicity studies provided a second line of evidence indicating the immunological mechanisms involved in the antitumor effects achieved by the combination of huKS1/4-IL-2 fusion protein and *mMIG* gene therapy (Fig. 7). Thus, splenocytes isolated from BALB/c mice 12 days after induction of pulmonary metastases with CT26-KSA-MIG tumor cells and subsequent treatment with huKS1/4-IL-2 fusion protein specifically lysed ≤44% of CT26-KSA tumor target cells. In contrast, only 29% lysis of target cells was achieved by splenocytes obtained from mice treated with *mMIG* gene therapy alone ($P < 0.001$). Furthermore, the involvement of MHC class I antigen restricted $CD8^+$ T-effector cells was clearly indicated by a specific inhibition of cytotoxicity. Thus, tumor target cell lysis was essentially abrogated when splenocytes were coincubated with an anti-MHC class I antibody and decreased to only 22% when coincubated with an anti-MHC class II antibody ($P < 0.001$), suggesting a helper effect of $CD4^+$ T cells.

DISCUSSION

We hypothesized that *MIG* (CXCL9) chemokine gene therapy aided by small but noncurative doses of huKS1/4-IL-2 might be effective in suppressing s.c. growth of murine colon carcinoma and inhibiting their pulmonary metastases. The rationale for this type of tumor immunotherapy is first to induce chemoattraction of immune effector cells to the tumor microenvironment by *MIG* chemokine gene therapy and then to activate these cells at the tumor site with an antibody-IL-2 fusion protein.

Here, we demonstrate that the combination of a noncurative dose of huKS1/4-IL-2 fusion protein with *mMIG* chemokine-based gene therapy is far superior to the antitumor effect achieved by either therapy alone at these dose levels. In fact, this combination therapy is more effective in markedly decreasing s.c. CT26-KSA colon carcinoma tumor growth as well as in suppressing the dissemination of established pulmonary metastases, resulting in a ≤4-fold prolongation of life span. The antitumor effect achieved in this murine colon carcinoma model is based primarily on immunological mechanisms involving the chemoattraction and subsequent activation of both $CD8^+$ and $CD4^+$ T lymphocytes, combined with an angiostatic effect induced by murine MIG.

These conclusions are supported by four lines of evidence. First, the treatment effect of the combination therapy was specifically abrogated in mice depleted of $CD8^+$ cells and markedly suppressed in mice depleted of $CD4^+$ T lymphocytes. Second, cytotoxicity studies indicated the involvement of MHC class I antigen-restricted $CD8^+$ and MHC class II antigen-restricted $CD4^+$ T cells. Third, immunohistochemical analyses demonstrated infiltration of tumor tissues by both $CD8^+$ and $CD4^+$ T cells. Fourth, an angiostatic effect of MIG was indicated by H&E staining and immunohistochemical analyses of Matrigel-embedded tumor cells, and by hemoglobin measurements.

Only a limited number of studies have thus far analyzed the role of chemokines in cancer immunotherapy. Specifically, the role of *MIG* gene therapy was investigated in two studies. First, in an immunodeficient (SCID) mouse model of human non-small cell lung carcinoma A549 (32), intratumoral injections of recombinant human MIG (rhMIG) or a recombinant adenoviral vector encoding the human *MIG* gene resulted in suppression of s.c. tumor growth in SCID mice. This effect was thought to be attributable to a decrease in tumor-derived blood vessel growth but was not accompanied by significantly increased numbers of tumor-infiltrating neutrophils or macrophages. The second study (20), in a model of human Burkitt's lymphoma CA46 in immunodeficient BALB/c *nu/nu* mice, demonstrated that s.c. tumor growth could be suppressed, although not completely halted; however, this antitumor effect could be achieved only by intratumoral injections using a combination therapy of EBV-immortalized human lymphocytes and rhMIG. These results were mainly attributed to extensive tumor necrosis, including marked vascular damage and intravascular thrombosis but without any apparent difference in lymphocyte, neutrophil, or monocyte infiltration compared with controls.

In contradistinction, our own study used a syngeneic immunocompetent model of murine colon carcinoma, which allows the critical evaluation of immune effector functions induced by chemokine gene therapy, that are likely among the most important biological properties of chemokines. Furthermore, our survival studies are based on the growth and dissemination of pulmonary metastases and, thus, mimic a clinical setting much more closely than the correlation of life span with the growth of s.c. tumors.

To our knowledge, only one other study examined the effects of *MIG* chemokine gene therapy combined with cytokine gene therapy. In this case, cDNA for both mMIG and mIL12 were encoded in the same recombinant adenoviral vector and applied by intratumoral injections to a s.c. syngeneic model of murine mammary adenocarcinoma PyMT (33). The combination of both gene therapies only slightly improved the growth delay achieved with either gene therapy alone, and <50% of animals achieved a 2-fold increase in life span.

The results of our study clearly demonstrate that the combined application of *mMIG* gene therapy with an antibody-IL-2 fusion protein targeted to the tumor microenvironment is superior in its antitumor effects to the application of these respective agents alone. In addition, a critical feature of our approach is the tumor-targeting of IL-2 with a recombinant antibody cytokine fusion protein, which takes advantage of the paracrine nature of IL-2 to locally activate those T cells that were specifically chemoattracted to the tumor microenvironment by *MIG* gene therapy. This maneuver resulted in an increase in life span and, importantly, in an abrogation of disseminated pulmonary metastases as well as a marked suppression of s.c. tumor growth. Furthermore, by targeting small doses of IL-2 to the tumor microenvironment, we reduce potentially dose-limiting toxicities of systemic IL-2 administration. In this regard, we demonstrated previously that huKS1/4-IL-2 fusion protein administered at high dose levels (7×15 μg) can eradicate experimental metastases of CT26-KSA colon carcinoma. In contrast, the application of a suboptimal dose (6×5 μg) did not inhibit tumor growth (22). However, by adding chemokine gene therapy to the already established IL-2 fusion protein treatment we

were able to significantly lower the dose of fusion protein required to achieve antitumor effects in mice. Taken together, these findings are of potential importance for future clinical applications where minimal amounts of optimally effective cytokines or chemokines are crucial in avoiding toxicities caused by these potent immune stimulators and in achieving successful cancer immunotherapy.

ACKNOWLEDGMENTS

We thank Dr. Lili Feng, The Scripps Research Institute, for providing polyclonal rabbit anti-mMig antibody and Collette Beaton for the preparation of this manuscript.

REFERENCES

1. Rodolfo, M., and Colombo, M. P. Interleukin-12 as an adjuvant for cancer immunotherapy. Methods (Orlando), *19:* 114–120, 1999.
2. Clinton, S. K., Canto, E., and O'Donnell, M. A. Interleukin-12. Opportunities for the treatment of bladder cancer. Urol. Clin. N. Am., *27:* 147–155, 2000.
3. Margolin, K. A. Interleukin-2 in the treatment of renal cancer. Semin. Oncol., *27:* 194–203, 2000.
4. Gollob, J. A., Mier, J. W., Veenstra, K., McDermott, D. F., Clancy, D., Clancy, M., and Atkins, M. B. Phase I trial of twice-weekly intravenous interleukin 12 in patients with metastatic renal cell cancer or malignant melanoma: ability to maintain IFN-γ induction is associated with clinical response. Clin. Cancer Res., *6:* 1678–1692, 2000.
5. Tahara, H., and Lotze, M. T. Antitumor effects of interleukin-12 (IL-12): applications for the immunotherapy and gene therapy of cancer. Gene Ther., *2:* 96–106, 1995.
6. Schmidinger, M., Steger, G. G., Wenzel, C., Locker, G. J., Brodowicz, T., Budinsky, A. C., Wiltschke, C., Kramer, G., Marberger, M., and Zielinski, C. C. Sequential administration of interferon γ and interleukin-2 in metastatic renal cell carcinoma: results of a phase II trial. Austrian Renal Cell Carcinoma Study Group. Cancer Immunol. Immunother., *49:* 395–400, 2000.
7. Bukowski, R. M. Cytokine combinations: therapeutic use in patients with advanced renal cell carcinoma. Semin. Oncol., *27:* 204–212, 2000.
8. Keilholz, U., and Eggermont, A. M. The emerging role of cytokines in the treatment of advanced melanoma. For the EORTC Melanoma Cooperative Group. Oncology, *58:* 89–95, 2000.
9. Wang, J. M., Deng, X., Gong, W., and Su, S. Chemokines and their role in tumor growth and metastasis. J. Immunol. Methods, *220:* 1–17, 1998.
10. Oppenheim, J. J., Murphy, W. J., Chertox, O., Schirrmacher, V., and Wang, J. M. Prospects for cytokine and chemokine biotherapy. Clin. Cancer Res., *3:* 2682–2686, 1997.
11. Hogaboam, C. M., Bone-Larson, C., Matsukawa, A., Steinhauser, M. L., Blease, K., Lukacs, N. W., and Kunkel, S. L. Therapeutic use of chemokines. Curr. Pharm. Des., *6:* 651–663, 2000.
12. Rollins, B. J. Chemokines. Blood, *90:* 909–928, 1997.
13. Rossi, D., and Zlotnik, A. The biology of chemokines and their receptors. Annu. Rev. Immunol., *18:* 217–242, 2000.
14. Zlotnik, A., and Yoshie, O. Chemokines: a new classification system and their role in immunity. Immunity, *12:* 121–127, 2000.
15. Farber, J. M. HuMig: a new human member of the chemokine family of cytokines. Biochem. Biophys. Res. Commun., *192:* 223–230, 1993.
16. Farber, J. M. Mig and IP-10: CXC chemokines that target lymphocytes. J. Leukoc. Biol., *61:* 246–257, 1997.
17. Liao, F., Rabin, R. L., Yannelli, J. R., Koniaris, L. G., Vanguri, P., and Farber, J. M. Human Mig chemokine: biochemical and functional characterization. J. Exp. Med., *182:* 1301–1314, 1995.
18. Gasperini, S., Marchi, M., Calzetti, F., Laudanna, C., Vicentini, L., Olsen, H., Murphy, M., Liao, F., Farber, J., and Cassatella, M. A. Gene expression and production of the monokine induced by IFN-γ (MIG), IFN-inducible T cell α chemoattractant (I-TAC), and IFN-γ-inducible protein-10 (IP-10) chemokines by human neutrophils. J. Immunol., *162:* 4928–4937, 1999.
19. Strieter, R. M., Polverini, P. J., Kunkel, S. L., Arenberg, D. A., Burdick, M. D., Kasper, J., Dzuiba, J., Van Damme, J., Walz, A., and Marriott, D. The functional role of the ELR motif in CXC chemokine-mediated angiogenesis. J. Biol. Chem., *270:* 27348–27357, 1995.
20. Sgadari, C., Farber, J. M., Angiolillo, A. L., Liao, F., Teruya-Feldstein, J., Burd, P. R., Yao, L., Gupta, G., Kanegane, C., and Tosato, G. Mig, the monokine induced by interferon-γ, promotes tumor necrosis *in vivo*. Blood, *89:* 2635–2643, 1997.
21. Loetscher, M., Gerber, B., Loetscher, P., Jones, S. A., Piali, L., Clark-Lewis, I., Baggiolini, M., and Moser, B. Chemokine receptor specific for IP10 and mig: structure, function, and expression in activated T-lymphocytes. J. Exp. Med., *184:* 963–969, 1996.
22. Xiang, R., Lode, H. N., Dolman, C. S., Dreier, T., Varki, N. M., Qian, X., Lo, K. M., Lan, Y., Super, M., Gillies, S. D., and Reisfeld, R. A. Elimination of established murine colon carcinoma metastases by antibody-interleukin 2 fusion protein therapy. Cancer Res., *57:* 4948–4955, 1997.
23. Xiang, R., Lode, H. N., Dreier, T., Gillies, S. D., and Reisfeld, R. A. Induction of persistent tumor-protective immunity in mice cured of established colon carcinoma metastases. Cancer Res., *58:* 3918–3925, 1998.
24. Xiang, R., Lode, H. N., Gillies, S. D., and Reisfeld, R. A. T cell memory against colon carcinoma is long-lived in the absence of antigen. J. Immunol., *163:* 3676–3683, 1999.
25. Kozak, M. Downstream secondary structure facilitates recognition of initiator codons by eukaryotic ribosomes. Proc. Natl. Acad. Sci. USA, *87:* 8301–8305, 1990.
26. Kozak, M. An analysis of vertebrate mRNA sequences: intimations of translational control. J. Cell Biol., *115:* 887–903, 1991.
27. Gillies, S. D., Lan, Y., Wesolowski, J. S., Qian, X., Reisfeld, R. A., Holden, S., Super, M., and Lo, K. M. Antibody-IL-12 fusion proteins are effective in SCID mouse models of prostate and colon carcinoma metastases. J. Immunol., *160:* 6195–6203, 1998.
28. Gillies, S. D., Lo, K. M., and Wesolowski, J. High-level expression of chimeric antibodies using adapted cDNA variable region cassettes. J. Immunol. Methods, *125:* 191–202, 1989.
29. Gillies, S. D., Reilly, E. B., Lo, K. M., and Reisfeld, R. A. Antibody-targeted interleukin 2 stimulates T-cell killing of autologous tumor cells. Proc. Natl. Acad. Sci. USA, *89:* 1428–1432, 1992.
30. Passaniti, A., Taylor, R. M., Pili, R., Guo, Y., Long, P. V., Haney, J. A., Pauly, R. R., Grant, D. S., and Martin, G. R. A simple, quantitative method for assessing angiogenesis and antiangiogenic agents using reconstituted basement membrane, heparin, and fibroblast growth factor. Lab. Investig., *67:* 519–528, 1992.
31. Drabkin, D. L., and Austin, J. H. Spectrophotometric constants for common hemoglobin derivatives in human, dog and rabbit blood. J. Biol. Chem., *98:* 719–724, 1932.
32. Addison, C. L., Arenberg, D. A., Morris, S. B., Xue, Y. Y., Burdick, M. D., Mulligan, M. S., Iannettoni, M. D., and Strieter, R. M. The CXC chemokine, monokine induced by interferon-γ, inhibits non-small cell lung carcinoma tumor growth and metastasis. Hum. Gene Ther., *11:* 247–261, 2000.
33. Palmer, K., Hitt, M., Emtage, P. C., Gyorffy, S., and Gauldie, J. Combined CXC chemokine and interleukin-12 gene transfer enhances antitumor immunity. Gene Ther., *8:* 282–290, 2001.